Hole transport and electrical properties in poly(p-phenylene vinylene):methanofullerene bulk-heterojunction solar cells

Y. GUO, L. G. WANG[*], T. X. ZHANG, D. L. XIE
School of Electrical Engineering and Automation, Henan Polytechnic University, Jiaozuo, 454000, People's Republic of China

The dependence of the hole transport and electrical properties of OC_1C_{10}-PPV:PCBM (poly(2-methoxy-5-(3',7'-dimethyloctyloxy)-p-phenylene vinylene):methanofullerene [6,6]-phenyl C_{61}-butyric acid methyl ester)-based bulk-heterojunction solar cells on their composition has been investigated. It is demonstrated that the current density versus voltage ($J-V$) characteristics of OC_1C_{10}-PPV:PCBM devices can be accurately described by using our recently introduced mobility model. Furthermore, we find that the width of the Gaussian density of states σ and hole zero-field mobilities in blends of OC_1C_{10}-PPV:PCBM are a function of PCBM weight percentage. The hole mobilities gradually increase with increasing fullerene concentration, whereas the values of the width of the Gaussian density of states σ gradually decrease with increasing fullerene concentration. In addition, it is shown that the boundary carrier density of OC_1C_{10}-PPV:PCBM-based devices has an important effect on the $J-V$ characteristics, and the variation of voltage with boundary carrier density is dependent on the current density.

1. Introduction

Organic solar cells based on thin films of conjugated polymer/fullerene bulk-heterojunction are a promising system for converting solar energy into electricity [1-3]. These systems open up a wide field of applications due to their light weight, low cost, ease of processing, and mechanical flexibility. A promising organic solar cell candidate is based on the conjugated polymer poly (2-methoxy-5-(3',7'-dimethyloctyloxy)-p-phenylene vinylene) (OC_1C_{10}-PPV) as electron donor and the methanofullerene [6,6]-phenyl C_{61}-butyric acid methyl ester (PCBM) as electron acceptor, exhibiting power conversion efficiencies of around 3 % under air mass (AM) 1.5 illumination [4, 5]. In this kind of organic photovoltaic cells, photon absorption in bulk-heterojunction mainly creates excited electron–hole pairs that subsequently dissociate at the heterojunction interface via an ultrafast charge transfer from the donor to the acceptor [6, 7]. These photogenerated free holes and electrons are then transported through the donor and acceptor phases towards the anode and cathode, respectively, resulting in an external photocurrent density. As a result, the external photocurrent does not solely depend on the photogeneration rate of free holes and electrons, but also on the transport properties of the holes and electrons in the organic materials. Therefore, knowledge about the charge transport properties of the individual components and OC_1C_{10}-PPV:PCBM blends is indispensable for further improvement of the performance of organic photovoltaic devices based on OC_1C_{10}-PPV:PCBM heterojunction.

For pure OC_1C_{10}-PPV, the transport of holes has been extensively studied in polymer light-emitting diodes and a hole mobility of $5\times10^{-11}m^2/Vs$ has been obtained at room temperature [8-10]. For pure PCBM, the electron transport has also been investigated and an electron mobility of $2\times10^{-7}m^2/Vs$ has been obtained at room temperature [11]. However, the transport of separate charge carriers in OC_1C_{10}-PPV:PCBM blends may be different than the transport in individual compounds. In OC_1C_{10}-PPV:PCBM blends, light is mainly absorbed in the OC_1C_{10}-PPV, whereas the PCBM plays the role of electron acceptor and electron transport material. However, to obtain the maximum device efficiency, up to 80 wt.-% PCBM has to be added into the OC_1C_{10}-PPV:PCBM mixture [12]. It is not fully clear that why it is necessary to add relatively large amount of a material that barely contributes to the absorption of light in order to achieve optimal performance.

Understanding the fundamental questions concerning the operation of OC_1C_{10}-PPV:PCBM heterojunction solar cells and the processes limiting their performance is of crucial importance for the further advancement of these devices. Recently, we have developed a device model in

which the mobility depends on the temperature, electric field, and carrier density [13]. It has been demonstrated that the mobility model can rather well describe the charge transport in various organic materials [14-16]. Herein, we will apply the mobility model to calculate the current density versus voltage ($J-V$) characteristics and the variation of $J-V$ characteristics with the boundary carrier density of a series of devices of different OC_1C_{10}-PPV:PCBM compositions.

2. Model and methods

From a numerical solution of the master equation for hopping transport in a disordered energy system with a Gaussian density of states, Pasveer *et al.* obtained a unified description of the dependence of the mobility μ on the temperature T, electric field E, carrier density p [9]. However, it should be noted that their model, having a non-Arrhenius temperature dependence $\ln(\mu) \propto 1/T^2$, can only well describe the charge transport at low carrier densities. In order to better describe the charge transport, we extended their model to higher carrier densities by taking both the Arrhenius temperature dependence $\ln(\mu) \propto 1/T$ and non-Arrhenius temperature dependence into account. The improved mobility model can be described as follows [13]:

$$\mu(T,p) = \mu_0(T)\exp[\frac{1}{2}(\hat{\sigma}^2 - \hat{\sigma})(2pa^3)^\delta], \quad (1a)$$

$$\mu_0(T) = \mu_0 c_1 \exp(c_2\hat{\sigma} - c_3\hat{\sigma}^2), \quad (1b)$$

$$\delta \equiv 2\frac{\ln(\hat{\sigma}^2 - \hat{\sigma}) - \ln(\ln 4)}{\hat{\sigma}^2}, \quad \mu_0 \equiv \frac{a^2 v_0 e}{\sigma}, \quad (1c)$$

with $c_1 = 0.48 \times 10^{-9}$, $c_2 = 0.80$, and $c_3 = 0.52$. Where $\mu_0(T)$ is the mobility in the limit of zero carrier density and electric field, $\hat{\sigma} \equiv \sigma/k_B T$ is the dimensionless disorder parameter, σ is the width of the Gaussian density of states (DOS), a is the lattice constant, e is the charge of the carriers, and v_0 is the attempt frequency.

$$\mu(T,p,E) = \mu(T,p)^{g(T,E)}\exp[c_4(g(T,E)-1)], \quad (2)$$

$$g(T,E) = [1 + c_5(Eea/\sigma)^2]^{-1/2}, \quad (3)$$

where $g(T,E)$ is a weak density dependent function, c_4 and c_5 are weak density dependent parameters, given by

$$c_4 = d_1 + d_2\ln(pa^3) \quad (4a)$$

$$c_5 = 1.16 + 0.09\ln(pa^3) \quad (4b)$$

$$d_1 = 28.7 - 36.3\hat{\sigma}^{-1} + 42.5\hat{\sigma}^{-2} \quad (5a)$$

$$d_2 = -0.38 + 0.19\hat{\sigma} + 0.03\hat{\sigma}^2 \quad (5b)$$

Using the above improved mobility model and following coupled equations, the $J-V$ characteristics and other electrical properties of the bulk-heterojunction solar cells can be calculated by employing a particular uneven discretization method introduced in our previous papers [17, 18].

$$J = p(x)e\mu(T,p(x),E(x))E(x), \quad (6a)$$

$$\frac{dE}{dx} = \frac{e}{\varepsilon_0\varepsilon_r}p(x), \quad (6b)$$

$$V = \int_0^L E(x)dx, \quad (6c)$$

where x is the distance from the injecting electrode, L is the organic materials layer thickness sandwiched between two electrodes, ε_0 is the vacuum permeability, and ε_r is the relative dielectric constant of the organic materials.

3. Results and discussion

Using the improved mobility model and distinctive numerical calculation method as described in section 2, we now perform a systematic study for the hole transport and electrical properties of OC_1C_{10}-PPV:PCBM heterojunction solar cells. The solution of the coupled equations with the improved mobility model and the experimental $J-V$ measurements from Ref. [9] for pure OC_1C_{10}-PPV hole-only device is displayed in Fig. 1. It can be seen from the figure that the temperature dependent $J(V)$ curves can be excellently described using a single set of parameters, $\sigma = 0.131$ eV, $a = 1.4$ nm, and $\mu_0 = 1500$ m²/Vs. The parameters σ, a and μ_0 are determined by using a way that an optimal fit is obtained. As for the parameters, it is found that a relatively low a value leads to a relatively low σ value and gives rise to a good description of the experimental $J(V)$ curves in the low-field and density regime, whereas a relatively high a value leads to a relatively high σ value and gives rise to good fits mainly in the high-field and density regime. The parameter μ_0 decreases with decreasing a and σ, and increases with increasing a and σ. In addition, it is worth noting that the value of the disorder parameter σ (0.131 eV) for OC_1C_{10}-PPV in this study, is close to the value used by Pasveer *et al.*, and is striking similarity to the results obtained by van Mensfoort *et al.* (0.13 eV) [9, 19]. The value of the lattice constants a obtained in this work (1.4 nm) is smaller than the results obtained by Pasveer et al. (1.6 nm) [9]. These values of the

parameters demonstrate that the lower value of σ can be mainly attributed to the omission of the p dependence and the lower value of a can be mainly attributed to the overestimation of the E dependence.
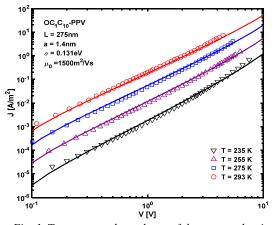

Fig. 1. Temperature dependence of the current density versus voltage characteristics of pure OC_1C_{10}-PPV device with a layer thickness of 275 nm. Symbols are experimental data from Ref. [9]. Lines are the numerically calculated results from Eqs. (1) – (6).

Fig. 2 shows the dark current density versus voltage ($J – V$) characteristics of OC_1C_{10}-PPV:PCBM blends that were measured and calculated in hole-only devices for different wt.-% of PCBM. For clarity, the pure OC_1C_{10}-PPV and three compositions of device (33, 50, 80 wt.-% of PCBM) are shown in (a), (b), (c), and (d), respectively. The values of the width of the DOS σ obtained in this work are 0.131 eV, 0.13 eV, 0.12 eV and 0.11 eV for OC_1C_{10}-PPV:PCBM blends with 0, 33, 50, 80 wt.-% of PCBM, respectively. It appears from the figure that our simulated results are in fairly good agreement with the original experiment data for the entire range of applied fields. This demonstrates that our improved model is applicable to the hole transport in OC_1C_{10}-PPV:PCBM bulk-heterojunction solar cells. The width of the DOS σ and calculated hole zero-field mobilities in blends of OC_1C_{10}-PPV:PCBM are presented as a function of wt.-% PCBM in Fig.3. It can be observed from the figure that the hole mobility gradual increase with increasing fullerene concentration, while the values of the DOS σ gradual decrease with increasing fullerene concentration. Intuitively, one would expect that the hole transport properties of OC_1C_{10}-PPV:PCBM blends decrease with increasing fullerene concentration. However, from 33 to 80 wt.-% PCBM, the hole mobility of OC_1C_{10}-PPV:PCBM blends increase by more than two orders of magnitude. Accordingly, the values of the DOS σ decrease from 0.13 eV (33 wt.-%) to 0.11 eV (80 wt.-%). For this strong increase of the hole mobility, it has been proposed that the change in film morphology upon adding PCBM concentration results in an enhanced intermolecular interaction and, hence, in an improved

charge transfer between polymer molecules [21, 22]. Furthermore, due to the decrease of energetic disorder and likely the better ordering in the solid state, the use of a polymer with a high degree of regularity can significantly increase the mobility, which favors charge delocalization. As a result, the molecular conformation and weakly ordered stacking of the molecules should be the origin of the poor hole transport properties in pure OC_1C_{10}-PPV. However, upon blending OC_1C_{10}-PPV with PCBM, an improvement in the hole transport properties can be expected, resulting from the modifying molecular conformation or the lower disorder energy.
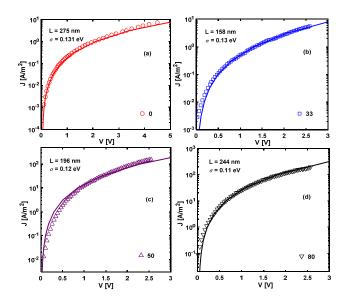

Fig. 2. The dark current density versus voltage characteristics of OC_1C_{10}-PPV:PCBM hole-only devices with varying wt.-% PCBM. Symbols are experimental data from Ref. [9, 20]. Lines are the numerically calculated results from Eqs. (1) – (6).
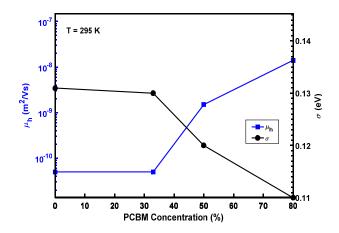

Fig. 3. The width of the DOS σ and hole zero-field mobilities μ_h in blends of OC_1C_{10}-PPV:PCBM as a function of PCBM weight percentage at room temperature. The mobilities are calculated from the space-charge limited current (SCLC) presented in Fig. 2.

As a next step, we further investigate the influence of the boundary carrier density $p(0)$ on the $J-V$ characteristics in OC_1C_{10}-PPV:PCBM heterojunction devices. The numerically calculated variation of $J-V$ characteristics with the boundary carrier density $p(0)$ for OC_1C_{10}-PPV:PCBM devices with different PCBM weight percentage and thicknesses at room temperature is plotted in Fig. 4. The figure shows that the voltage is an increasing function of the current density, and the variation of voltage with $p(0)$ is dependent on the current density. Too large or too small values of the boundary carrier density lead to incorrect $J-V$

characteristics, whereas the values of the boundary carrier density in the middle region can achieve reasonable results. In addition, it is clear that in order to reach the same current density J at the same $p(0)$, the weaker electric field and smaller voltage are needed in OC_1C_{10}-PPV:80 wt.-%PCBM device than those in OC_1C_{10}-PPV:33 wt.-%PCBM device. This further demonstrates that the hole transport properties of OC_1C_{10}-PPV:80 wt.-%PCBM blends is higher than that of OC_1C_{10}-PPV:33 wt.-%PCBM blends.
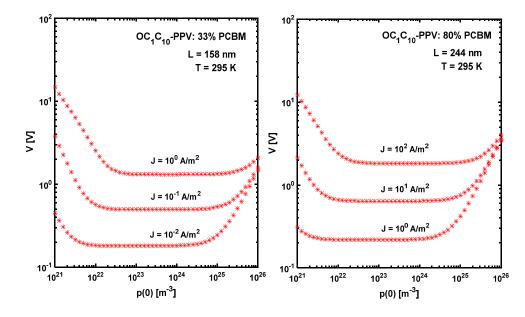

Fig. 4. Theoretical results of voltage versus the boundary carrier density of OC_1C_{10}-PPV:PCBM devices with different PCBM weight percentage and thicknesses at room temperature. Different Lines correspond to different current density values.

4. Summary and conclusions

In conclusion, the hole transport and electrical properties of OC_1C_{10}-PPV:PCBM heterojunction solar cells have been characterized. It is shown that the $J-V$ characteristics of the devices based on pure OC_1C_{10}-PPV and OC_1C_{10}-PPV:PCBM blends with varying PCBM concentrations can be accurately described by using the improved mobility model. The hole mobilities in OC_1C_{10}-PPV:PCBM blends increase with increasing fullerene concentration, whereas the values of DOS decrease with increasing fullerene concentration. This enhancement of the hole mobility with increasing fullerene concentration is strongly related to the optimization of the molecular conformation and a lower disorder energy. In addition, too large or too small values of the boundary carrier density lead to incorrect $J-V$ characteristics in OC_1C_{10}-PPV:PCBM heterojunction solar cells. These results open the prospect that our improved model is also applicable to the charge transport in PPV:PCBM-based bulk-heterojunction solar cells.

References

[1] C. J. Brabec, N. S. Sariciftci, J. C. Hummelen, Adv. Funct. Mater. **11**, 15 (2001).
[2] N. Kaura, M. Singhb, D. Pathakc, T. Wagnerc, J. M. Nunzi, Synth. Met. **190**, 20 (2014).
[3] F. Laquai, D. Andrienko, R. Mauer, P. W. M. Blom, Macromol. Rapid Commun. **36**, 1001 (2015).
[4] S. E. Shaheen, C. J. Brabec, N. S. Sariciftci, F. Padinger, T. Fromherz, J. C. Hummelen, Appl. Phys. Lett. **78**, 841 (2001).
[5] M. M. Wienk, J. M. Kroon, W. J. H. Verhees, J. Knol, J. C. Hummelen, P. A. van Hal, R. A. J. Janssen, Angew. Chem. Int. Ed. **42**, 3371 (2003).

[6] N. S. Sariciftci, L. Smilowitz, A. J. Heeger, F. Wudl, Science **258**, 1474 (1992).

[7] C. J. Brabec, G. Zerza, G. Cerullo, S. De Silvestri, S. Luzzati, J. C. Hummelen, S. Sariciftci, Chem. Phys. Lett. **340**, 232 (2001).

[8] P. W. M. Blom, M. J. M. de Jong, M. G. van Munster, Phys. Rev. B **55**, R656 (1997).

[9] W. F. Pasveer, J. Cottaar, C. Tanase, R. Coehoorn, P. A. Bobbert, P. W. M. Blom, D. M. deLeeuw, M. A. J. Michels, Phys. Rev. Lett. **94**, 206601 (2005).

[10] L. G. Wang, H. W. Zhang, X. L. Tang, C. H. Mu, J. Li, Curr. Appl. Phys. **10**, 1182 (2010).

[11] V. D. Mihailetchi, J. K. J. van Duren, P. W. M. Blom, J. C. Hummelen, R. A. J. Janssen, J. M. Kroon, M. T. Rispens, W. J. H. Verhees, M. M. Wienk, Adv. Funct. Mater. **13**, 43 (2003).

[12] V. D. Mihailetchi, H. Xie, B. de Boer, L. J. Koster, P. W. M. Blom, Adv. Funct. Mater. **16**, 699 (2006).

[13] L. G. Wang, H. W. Zhang, X. L. Tang, C. H. Mu, Eur. Phys. J. B **74**, 1 (2010).

[14] L. G. Wang, H. W. Zhang, X. L. Tang, Y. Q. Song, Z. Y. Zhong, Y. X. Li, Phys. Scr. **84**, 045701 (2011).

[15] I. Katsouras, A. Najafi, K. Asadi, A. J. Kronemeijer, A. J. Oostra, L. J. A. Koster, D. M. de Leeuw, P. W. M. Blom, Org. Electron. **14**, 1591 (2013).

[16] L. G. Wang, Y. X. Gao, X. L. Liu, L. F. Cheng, J. Optoelectron. Adv. M. **18**(5-6), 504 (2016).

[17] L. G. Wang, H. W. Zhang, X. L. Tang, Y. Q. Song, Optoelectron. Adv. Mat. **5**(3), 263 (2011).

[18] M. L. Liu, L. G. Wang, J. Optoelectron. Adv. M. **19**, 406 (2017).

[19] S. L. M. van Mensfoort, S. I. E. Vulto, R. A. J. Janssen, R. Coehoorn, Phys. Rev. B **78**, 085208 (2008).

[20] V. D. Mihailetchi, L. J. Koster, P. W. M. Blom, C. Melzer, B. de Boer, J. K. J. van Duren, R. A. J. Janssen, Adv. Funct. Mater. **15**, 795 (2005).

[21] R. Pacios, D. D. C. Bradley, J. Nelson, C. J. Brabec, Synth. Met. **137**, 1469 (2003).

[22] C. Melzer, E. J. KOOP, V. D. Mihailetchi, P. W. M. Blom, Adv. Funct. Mater. **14**, 865 (2004).

*Corresponding author: wangliguo@hpu.edu.cn